Pressure Heating of Electrons in Capacitively Coupled rf Discharges

M. M. Turner
School of Physical Sciences, Dublin City University, Dublin, Ireland
(Received 28 March 1995)

Collisionless heating in low-pressure capacitively coupled rf discharges is usually attributed to a stochastic interaction between electrons and the oscillating sheath. We show that this explanation is not complete—there is a powerful heating mechanism associated with pressure effects that arise during the expansion and contraction of sheaths.

PACS numbers: 52.50.Gj, 52.65.–y, 52.75.–d

Capacitively coupled rf discharges have attracted attention for many years [1] because of their interesting physics and the existence of applications in areas like semiconductor materials processing [2]. The center of recent interest is the low-pressure regime where a variety of novel effects have been observed including collisionless heating, which is associated with the motion of the plasma sheaths as the rf current oscillates [1,3,4]. In an rf discharge, transient sheaths form on both electrodes. As the rf phase advances, the sheath on one electrode expands while the other collapses so that each sheath cyclically advances and retreats. Since the sheath voltage is generally much larger than the electron temperature T_e, the sheaths usually present an impenetrable potential barrier to electrons; electrons can escape to an electrode only when the adjacent sheath is fully collapsed, or nearly so. So when an electron strikes a sheath it will generally be reflected, and because of the sheath motion the electron energy will generally change on reflection. Although this change can be positive or negative, it can be shown under certain assumptions that the averaged effect is positive [1,5,6]. This heating mechanism is known as stochastic heating. There are several stochastic heating theories based on this "hard wall" view of the sheaths [1,5,6]; they differ in their detailed assumptions, and it is not clear which, if any, should be preferred, but the underlying model that we have just described is common and widely accepted. We show in this Letter that an important heating effect exists that falls outside the scope of the hard wall model and the theories derived from it. We first demonstrate that this heating is present and we then develop a quantitative theory to describe it. Our study uses results from a self-consistent kinetic simulation based on the well-known particle in cell algorithm, with Monte Carlo collisions (PIC-MCC) [7–9]. This technique has been successfully applied to many problems in low-temperature plasma physics, and has demonstrated remarkable precision in calculations of the exotic electron energy distribution functions that typically occur in low-pressure capacitively coupled discharges [4,10,11]. Our implementation is conventional; we use a one-dimensional explicit particle mover with ion subcycling where relevant. In the calculations reported here we used a set of electron and ion collision frequencies appropriate for argon gas at a pressure of 10 mTorr. Our choices of time step and cell size satisfy the usual accuracy and stability criteria, and we used $\sim 10^5$ particles, which is a few hundred per cell.

Our investigation begins by considering an archetypal collisionlessly excited rf discharge in argon [3,4,10]. We excite a model plasma using a fixed current density of amplitude 1 mA cm^{-2}, between electrodes separated by 5 cm. The electrodes are assumed perfectly absorbing of electrons and ions. This simulation reproduces the features that have been considered characteristic of collisionlessly dominated discharges in argon: heating concentrated at the plasma-sheath interface [4,10], negative heating in the bulk plasma [4,10], and a distinctive two-temperature electron energy distribution [3,4,10]. We will compare the results of this bounded simulation with a similar case with periodic boundary conditions. In the periodic model, the plasma density distribution is controlled by fixed positive charges which are placed to correspond with the ion density distribution from the bounded simulation, as shown in Fig. 1. This periodic system initially contains an equal amount of positive and negative charge, and is quasineutral everywhere, a state which we maintain by suppressing the creation of charged particles in "ionizing" collisions (we otherwise use identical collision handling). The periodic model closely resembles the bounded system when we drive it with the same current density [12], except that any collisionless heating cannot be stochastic heating owing to the absence of sheaths. However, the heating is not much diminished, and indeed all the above-mentioned characteristic features of the bounded system are preserved in the periodic analog, as we show for the heating in Fig. 1 and the electron energy distribution function in Fig. 2. This is a compelling demonstration that the hard wall stochastic heating model is insufficient. We next show that the nonstochastic collisionless heating that appears in the right half of Fig. 1 can be understood as a pressure effect connected with the compression and rarefaction of electrons as they flow in and out of the sheath regions (it is convenient to retain this term for the regions of lower density in the periodic system).

 0031-9007/95/75(7)/1312(4)$06.00

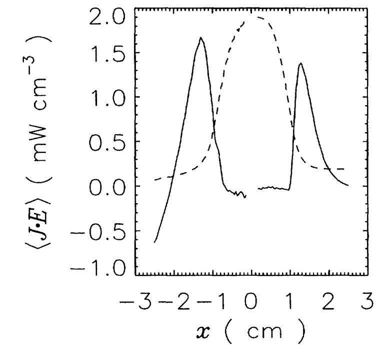

FIG. 1. A comparison of the time-averaged electron heating $\langle JE \rangle$ from a self-consistent simulation of a capacitively coupled rf discharge excited at $\omega_{\rm rf} = 2\pi \times 13.56$ MHz, in argon at 10 mTorr, with the results from the analogous periodic system discussed in the text. Both systems are current driven with an amplitude of 1 mA cm^{-2}. The solid line in the left half of the figure is the result of the bounded simulation; the solid line in the right half of the figure is the periodic result. The corresponding dashed lines show the self-consistently computed ion density profile and the model plasma density profile assumed in the periodic calculation (the maximum density in both cases is $\sim 10^9$ cm^{-3}). To facilitate the comparison, the $\langle JE \rangle$ data from the periodic system have been modified by discarding heating that occurs at times and in places where electrons are absent in the bounded calculation.

It has been noticed before that pressure effects explain the appearance of negative heating in the bulk plasma [4], and are associated with collisionless heating in the sheaths [13]. We argue here that pressure heating is a distinct mechanism, not a fluid representation of stochastic heating. The pressure effect in question is caused by the difference in plasma density and temperature between the bulk plasma and the sheath region. When a sheath expands, electrons flow into the adjacent bulk plasma and are compressed. At the same time, electrons are rarefied as they flow into the opposite collapsing sheath. Since the thermal conductivity of the bulk plasma is finite, these

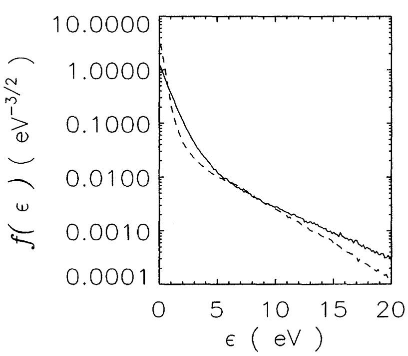

FIG. 2. A comparison of the electron energy distribution functions from the bounded simulation and the analogous periodic model system, for the same conditions as in Fig. 1. These data are time averaged at $x = 0$. The solid and dashed lines are from the bounded and periodic models, respectively.

simultaneous rarefaction and compression effects produce nonequilibrium thermal disturbances, and the net work being done is not necessarily zero, as we now show. The temperature variations in the plasma are described by the energy balance equation [13]

$$\frac{3}{2}\frac{\partial}{\partial t}(n_e k_B T_e) + \frac{5}{2}\frac{\partial}{\partial x}(u_e n_e k_B T_e) + \frac{\partial q_e}{\partial x} + u_e n_e e E + \frac{3}{2}\frac{n_e k_B T_e}{\tau_e} = 0, \quad (1)$$

where n_e, u_e, ν_e, and q_e are the electron density, drift velocity, collision frequency, and thermal flux, respectively, τ_e is a phenomenological energy relaxation time constant incorporating inelastic collisions, etc., and E is the electric field. The electric field may be removed from Eq. (1) using the momentum balance equation [13],

$$m_e n_e \frac{\partial u_e}{\partial t} + \frac{\partial}{\partial x}(n_e k_B T_e) + e n_e E + m_e n_e u_e \nu_e = 0. \quad (2)$$

We take it that $m_e u_e^2 \ll k_B T_e$, and, therefore, we have neglected terms in the drift energy. Our solution of Eq. (1) assumes that n_e is independent of time and that T_e can be separated into a time independent term $T_e^{(0)}$, and a term that oscillates with the rf, $T_e^{(1)}$. Our procedure is to express n_e and $T_e^{(0)}$ in terms of elementary functions and hence obtain a linearizable equation for the complex amplitude $T_e^{(1)}$. To complete the development, we approximate the time dependent part of the heat flux by

$$\frac{\partial q_e^{(1)}}{\partial x} = -n_e \bar{\kappa}_e \frac{\partial^2}{\partial x^2}(k_B T_e^{(1)}), \quad (3)$$

where $\bar{\kappa}_e = k_B \bar{T}_e^{(0)}/m_e \bar{\nu}_e$ is the time- and space-averaged electron thermal conductivity and ν_e is the electron collision frequency. With the analytically convenient and qualitatively plausible choices $T_e^{(0)}(x) = T_0 \cosh(x/x_1)$ and $n_e(x) = n_0 \mathrm{sech}(x/x_0)$, and after further manipulations involving the current continuity equation, the linearized equation for $T_e^{(1)}$ is

$$\frac{d^2}{dx^2}T_e^{(1)} - \alpha^2 T_e^{(1)} = \Gamma\left[(3x_0 + 2x_1)\sinh\frac{(x_0 + x_1)}{x_0 x_1}x + (3x_0 - 2x_1) \times \sinh\frac{(x_0 - x_1)}{x_0 x_1}x\right], \quad (4)$$

where $\alpha^2 = (3/2\bar{\kappa}_e)(1/\tau_e - i\omega_{\rm rf})$, $\Gamma = J_0 T_0/4 e n_0 \times \bar{\kappa}_e x_0 x_1$, and J_0 is the current density amplitude. There is no difficulty in solving Eq. (4); since the solution is odd, an appropriate boundary condition for a periodic system of length $2L$ is $T_e^{(1)}(\pm L) = 0$. We will not give the complete solution, since it is relatively cumbersome and not hard to derive. As Fig. 3 shows, the solutions are essentially thermal waves [14] driven by the modulation

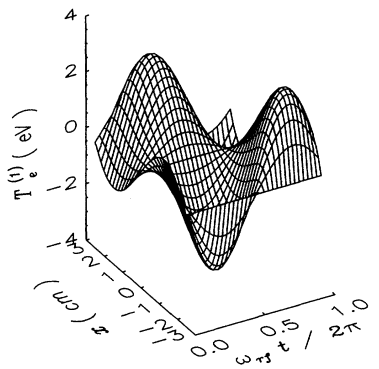

FIG. 3. A sample solution of Eq. (4) of the text, showing the thermal wave. The parameters (using symbols defined in the text) are $n_0 = 6 \times 10^8\ \mathrm{cm}^{-3}$, $J_0 = 1\ \mathrm{mA\,cm}^{-2}$, $T_0 = 3$ eV, $x_0 = 0.8$ cm, $x_1 = 0.9$ cm, $\omega_{\mathrm{rf}} = 2\pi \times 13.56$ MHz, $\bar{\nu}_e = 60$ MHz, and $L = 2.5$ cm. The phase is referenced to $J(t) = J_0 \sin \omega_{\mathrm{rf}} t$.

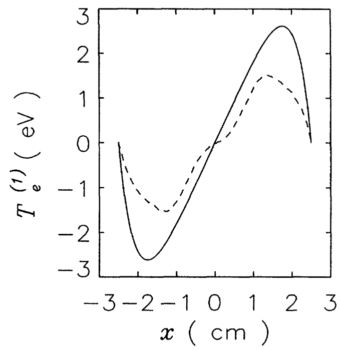

FIG. 4. Comparison of the amplitude of the thermal wave shown in Fig. 3 with results of a simulation for similar conditions. The solid and dashed lines are the results of the theory and the simulation, respectively.

of the electron temperature at the interface between the sheath region and the bulk plasma. Given $T_e^{(1)}$, we can recover the electric field from Eq. (2) and hence find the time-averaged heating using $\langle JE \rangle = \frac{1}{2}\mathrm{Re}\,(JE^*)$. A comparison between this theory and the simulation is of interest. For this calculation, we chose the plasma density in the simulation to have the form assumed above, and subsequently selected T_0 and x_1 to match the simulation results. In Figs. 4 and 5 we present comparisons between the theory and simulation for the conditions specified in the caption of Fig. 3. There is good qualitative and fair quantitative agreement, which persists over a variety of conditions different from those shown. A point of interest is that the theory predicts the region of negative heating at the center of the discharge [4]. This feature appears when the pressure-driven contribution to the current would exceed the total current if it were not opposed by an electric field. These data indicate that the theory captures the essential features of the pressure heating mechanism. With the restriction that $x_1 = x_0$, the expression for $\langle JE \rangle$ can be approximately integrated to give a compact formula for the space- and time-averaged power $\bar{P}$:

$$\bar{P} \approx \frac{J_0^2 x_0}{e^2 n_0}\left[\frac{5k_B T_0 \sinh(2L/x_0)}{32\bar{\kappa}_e(1+\beta^2)} + m_e \bar{\nu}_e \sinh(L/x_0)\right], \tag{5}$$

where the first term represents the pressure heating and the dimensionless parameter $\beta = 3\omega_{\mathrm{rf}} x_0^2/8\bar{\kappa}_e$ measures the importance of thermal conduction effects. The terms involving τ_e are not important in the pressure range of present concern. Equation (5) implies that the ratio of pressure heating to Ohmic heating is given by

$$\frac{\bar{P}_{\mathrm{pressure}}}{\bar{P}_{\mathrm{Ohmic}}} \approx \frac{5}{16}\frac{L}{x_0}(1+\beta^2)^{-1}, \tag{6}$$

so when $\beta \ll 1$, the ratio of pressure heating to Ohmic heating is determined solely by the form of the plasma density distribution.

Conventional fluid simulations based on the moment equations do not completely include collisionless heating [13,15], which seems surprising in view of the demonstration above that collisionless heating is not inherently a kinetic effect. The following argument shows that this apparent paradox can be resolved. Apart from the magnitude of the heating, the most striking difference between kinetic and fluid simulations appears in the time-averaged temperature distribution $T_e^{(0)}(x)$, which is peaked in the sheaths in kinetic simulations, but essentially uniform in fluid calculations [15]. In our theory we specified this quantity *a priori* to agree with the kinetic simulation result. Had we allowed it to be in agreement with typical fluid results [15], the predicted collisionless heating would have been much smaller. A correct calculation of $T_e^{(0)}(x)$ is therefore critical. Since $\langle JE \rangle$ is far from uniform, $T_e^{(0)}(x)$ is sensitive to the heat transport term q_e, which is conventionally computed from Eq. (3) or a similar ex-

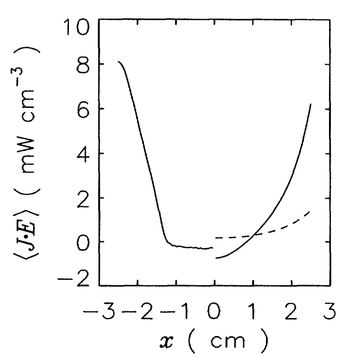

FIG. 5. Comparison of the time-averaged heating $\langle JE \rangle$ obtained from the periodic simulation (left half of the figure) with the result of the theory discussed in the text (right half of the figure). The dotted line in the right half of the figure is the Ohmic component of the heating calculated from the theory.

pression [13,15]. When the collision frequency is small, an unphysically large flux can result. This can be prevented by placing an upper bound on the thermal conductivity using the flux-limited electron diffusivity given by $D_e^{(\max)} = v_{\mathrm{th}}\Lambda$, where v_{th} is the electron thermal speed and $\Lambda = 2L/\pi$ is the diffusion length. The consequences of this correction are illustrated in a direct numerical solution of Eqs. (1) and (2), in which we finite differenced the spatial derivatives and performed a forward-marching time integration to find a harmonic steady state solution for $T_e(x,t)$, as in the kinetic calculations. We retained the formulation already discussed, except for the substitution of an Arrhenius-type expression [16] for the inelastic energy loss term in Eq. (1) and the insertion of a temperature-dependent collision frequency in Eq. (2). The results obtained in this way and shown in Fig. 6 are in fair agreement with the kinetic simulation of Fig. 5. So it seems that the absence of collisionless heating from fluid models is rooted in an overprediction of the heat flux that suppresses the thermal gradient across the plasma-sheath boundary.

In conclusion, we have shown that there is a powerful heating mechanism associated with pressure effects in capacitively coupled rf discharges, and we have presented a quantitative theory derived from the moment equations which is in good agreement with kinetic simulation results. The pressure heating effect persists in a periodic model system and it is, therefore, not connected with the presence of a sheath edge. These results are interesting and important because they contradict two widely held opinions: the non-Ohmic heating that occurs in rf discharges in intrinsically a kinetic effect, and the heating is predominantly associated with a stochastic interaction with the sheath edge.

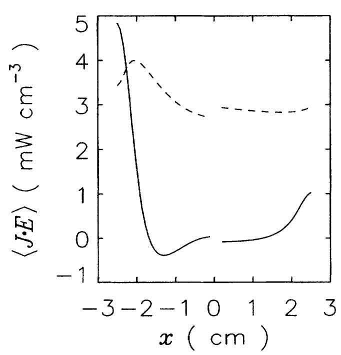

FIG. 6. Comparison of the numerical solutions of essentially Eqs. (1) and (2), with and without the flux-limited thermal conductivity. The left half of the figure shows the flux-limited case, the right half the conventional solution. Solid lines denote $\langle JE \rangle$ and dashed lines are $T_e^{(0)}(x)$ expressed in arbitrary units. In both cases $T_e^{(0)}(x=0) \approx 3$ eV. Except as noted in the text, the conditions are the same as in Figs. 3 and 5.

The author has benefited from several stimulating discussions on the topics of this Letter with Dr. D. Vender. This work was partially supported by EURATOM.

[1] V. A. Godyak, *Soviet Radio Frequency Discharge Research* (Delphic Associates, Inc., Falls Church, VA, 1986).
[2] D. B. Graves, IEEE Trans. Plasma Sci. **22**, 31 (1994).
[3] V. A. Godyak and R. B. Piejak, Phys. Rev. Lett. **65**, 996 (1990).
[4] M. Surendra and D. B. Graves, Phys. Rev. Lett. **66**, 1469 (1991).
[5] M. A. Lieberman, IEEE Trans. Plasma Sci. **16**, 638 (1988).
[6] I. D. Kaganovich and L. D. Tsendin, IEEE Trans. Plasma Sci. **20**, 86 (1992).
[7] C. K. Birdsall and A. B. Langdon, *Plasma Physics via Computer Simulation* (Adam Hilger, Bristol, 1991).
[8] R. W. Hockney and J. W. Eastwood, *Computer Simulation Using Particles* (Adam Hilger, Bristol, 1988).
[9] C. K. Birdsall, IEEE Trans. Plasma Sci. **19**, 65 (1991).
[10] V. Vahedi *et al.,* Plasma Sources Sci. Technol. **2**, 273 (1993).
[11] M. M. Turner and M. B. Hopkins, Phys. Rev. Lett. **69**, 3511 (1992).
[12] It is perhaps not well known that a periodic system can be driven; the technique is referred to in [7], Sec. 4.11 and Appendix D.
[13] M. Surendra and M. Dalvie, Phys. Rev. E **48**, 3914 (1993).
[14] L. D. Landau and E. M. Lifshitz, *Fluid Mechanics* (Pergamon Press, Oxford, 1978).
[15] T. E. Nitschke and D. B. Graves, J. Appl. Phys. **76**, 5646 (1994).
[16] M. Dalvie, M. Surendra, and G. S. Selwyn, Appl. Phys. Lett. **62**, 3207 (1993).